6 The impact of a negative global coupling on pattern formation during periodate reduction on Au(111) film electrodes

6.1 Introduction

As discussed in chapter 2, there are two main types of 'NDR' systems which give rise to instabilities in electrochemical systems: 'N-NDR' and 'S-NDR' systems. In chapter 5, pattern formation in an S-NDR system, namely the reduction of periodate on a Au electrode in the presence of camphor was studied, and it was discussed that the primary dynamic instability existing in this system is a Turing bifurcation giving rise to a stationary pattern. In fact, in chapter 4 (Fig. 4.15), it was also shown that the periodate/Au subsystem of this 'S-NDR' system possesses an N-shaped current–potential characteristics.

Studies on 'N-NDR' systems have dominated the field of nonlinear dynamics in electrochemical systems. In contrast to 'S-NDR' systems, they easily undergo oscillatory instabilities [13]. It has been demonstrated that in the presence of a so-called negative global coupling the emerging oscillations are often spatially inhomogeneous [19, 30]. A spatial coupling is called 'global' if a local fluctuation or perturbation is felt by all other positions with the same strength. In this case the dynamics depends on the spatial average of a system's variable. The global coupling is said to be positive if it has synchronizing effect which means that the coupling tends to damp spatial differences. However, the global coupling might also act in a way that the difference between the spatial average and the local value of the variable is enhanced and the coupling is towards destabilization of spatial homogeneous steady state. Such global coupling is called a negative global coupling.

In electrochemical systems a negative global coupling comes about if the RE is close to the WE [19, 30, 89]. That the position of the RE has an impact on pattern formation is easily understandable: The potential distribution in the electrolyte is decisively influenced by the potential distribution at its boundaries and thus also by the potential distribution at the electrode/electrolyte interface. A local change of the electrode potential affects the entire potential distribution within the electrolyte, whereby the value of the potential in the electrolyte is the more affected, the closer it is to the position of the electrode, at which the perturbation occurred. In a potentiostatic experiment, the externally applied voltage is composed of the voltage drop through the electrolyte between the WE and the RE and the double layer potentials at the WE and the RE (the latter represents, however, only a constant offset and can be neglected in all considerations on dynamic instabilities). A locally changed double layer potential at the WE thus also changes the potential at the position in the electrolyte, at which the RE probes the potential, for example, if a Haber-Luggin capillary is used at the tip of the capillary. This, in turn, causes the actual voltage difference between the WE and the RE to be different from the set one. As a consequence, the potentiostat changes the (Galvani) potential of the WE until actual and set voltage are equal again. A change of the potential of the WE affects the potential drop across the double layer at the entire electrode/electrolyte interface. This action represents a global coupling in the strict sense, if all positions of the WE have the same distance to the location of the RE, since only then the evolution equation of the double layer potential depends on the spatial average of the double layer potential. This is the case for a thin, quasi-1D ring electrode, if the RE is placed on the axis of the ring. For all other geometries, and in particular for all two-dimensional electrodes, the potential in the electrolyte at the position of the WE is a weighted average of the double layer potential distribution. And although a local change of the electrode potential causes the electrode potential to change at all positions, the strength of this coupling is different at different positions, and thus the coupling is nonlocal.

Until now, all studies on the impact of a negative global coupling on pattern formation in electrochemical systems were carried out with the above mentioned

geometries and relative arrangement of the WE and the RE, namely a thin ring electrode as WE and the RE positioned on the axis of ring [19-22, 30, 89-91].

A global coupling in electrochemical systems can also be achieved by inserting an ohmic resistance in series to the WE [92]. Here, the origin of the global coupling is even more apparent than in the case of the RE. The outer fixed voltage is now composed of the potential drop at the electrode/electrolyte interface at the WE, the potential drop through the electrolyte between the WE and the RE, and the potential drop across the external resistor. If the current density changes locally, the total current changes, and thus also the potential drop across the external resistor, which, since the sum over the three above mentioned potential drops is constant, causes a changed double layer potential drop at every position of the WE. Clearly, in this case the potential drop across the resistor depends on the global current and thus on the average double layer potential. Hence, a series resistor causes – independent of the geometry of the WE and independent of the relative arrangement of the WE and the RE – a global coupling in the strict sense. In contrast to the global coupling induced by a close RE, the global coupling caused by the external ohmic resistor is a positive global coupling [92]. However, there exist electronic devices that act like a negative ohmic resistance (Fig. 6.1) [93-95]. They were employed to compensate for the IR drop through the electrolyte [94] but also in studies on spatial instabilities of semiconductor devices [95]. If such a negative impedance device (NID) is inserted in series to the WE, it introduces a negative global coupling into the system.

In this chapter, we will employ an NID as shown in Fig. 6.1 to study the impact of a negative global coupling on pattern formation on two-dimensional, rectangular electrodes, a topic that was not addressed before. It is, however, of great importance since the same device is used to compensate the IR drop in potentiostatic circuits, and thus a negative global coupling is present in many electrochemical experiments. As a model system the periodate/Au system is used because the adsorption of a reaction intermediate causes a considerable shift of the surface plasmon resonance (cf. section 4.9). The system thus provides a sufficient contrast to monitor pattern formation with SPI.

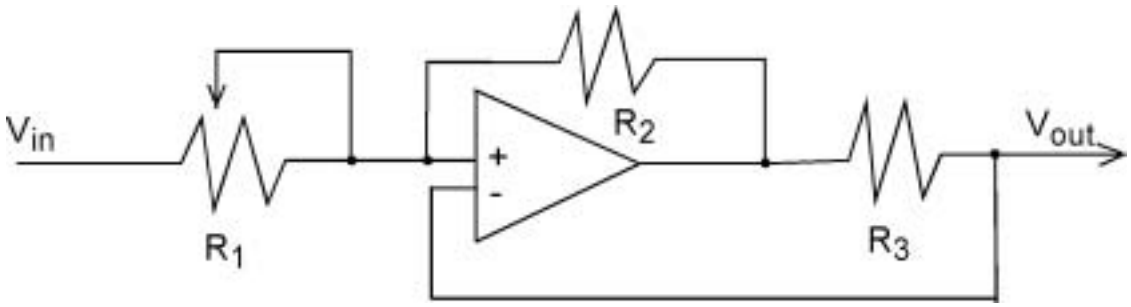

Figure 6.1: *Circuit of an electronic device with negative impedance ('negative impedance device'(NID)). Input and output voltage are related according to* $V_{out} = V_{in} + (R_1R_3/R_2)I$*, thus, the actual resistance of the NID is* $R_{NID} = (V_{in}-V_{out})/I = -R_1R_3/R_2$*, where* V_{out}*,* V_{in} *are the output, input voltage,* R_2*,* R_3*, the fixed normal resistors,* R_1*, the adjustable normal resistor, I, the current [93]. (In our experiments, the NID was connected to WE and potentiostat in series, the '*V_{in}*' end is connected to the WE and '*V_{out}*' to the potentiostat.)*

6.2 Results

a. Periodate reduction system without the NID

As previously seen in Fig. 4.15, the CV of periodate reduction on Au in concentrated perchlorate solution exhibits a region with an NDR of the 'N-type'. When increasing the series resistance, bistability and oscillations were found, as characteristic for all N-NDR systems (see chapter 2). A CV of periodate reduction in a 2 mM $NaClO_4$ solution and a total cell resistance of 1.0 kΩ is displayed in Fig. 6.2a. For this comparatively high series resistance, the bistable region is approximately 200 mV wide. During a voltage scan the current density overshoots the active branch during the passive–active transition. When holding the external voltage constant close to the active–passive transition, the current oscillates. A time series of these sustained oscillations is shown in Fig. 6.2b. The oscillations were only observed when the voltage scan was stopped during a scan from negative to positive potentials, but never, when a negative potential scan was interrupted.

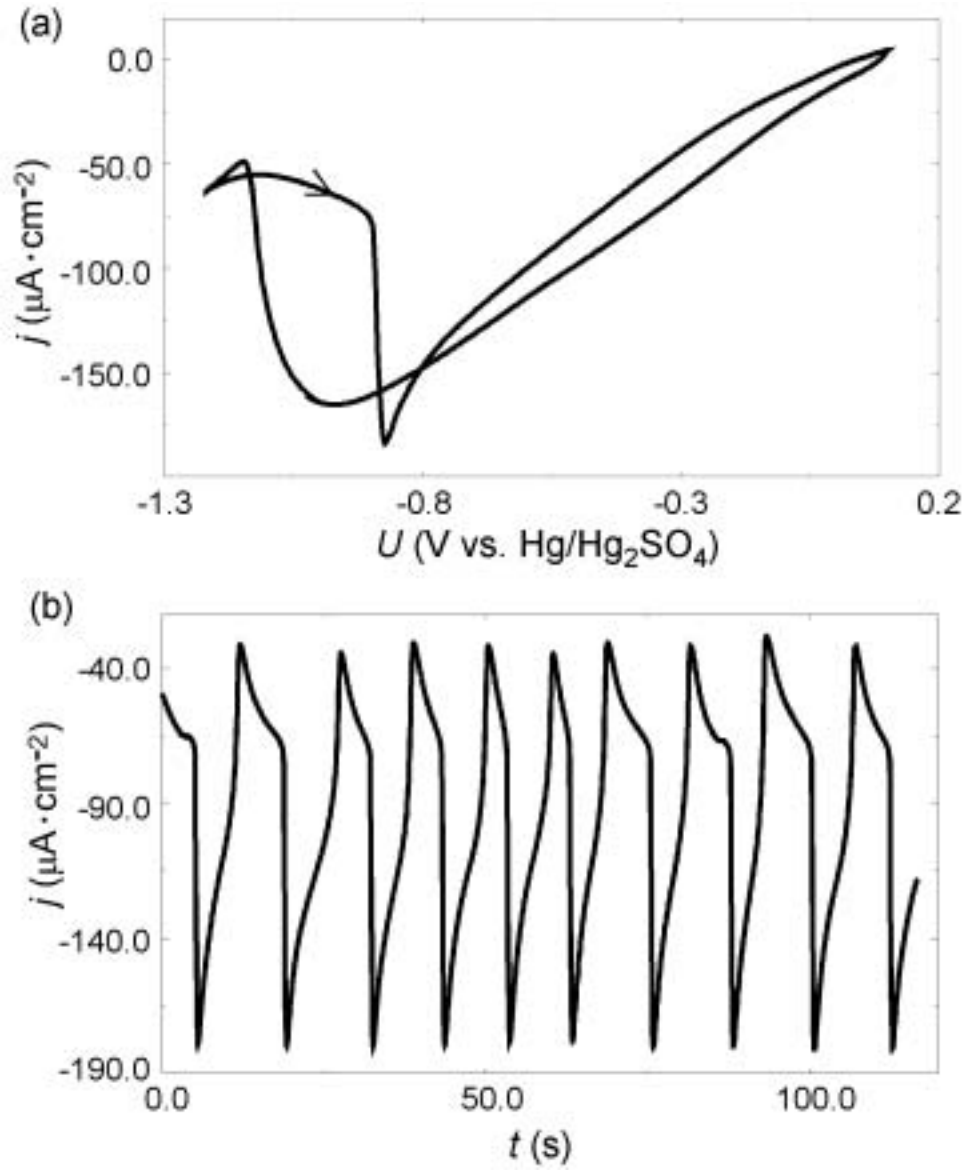

Figure 6.2: *(a) Cyclic voltammogram of periodate reduction on a Au(111) film electrode (scan rate, 50 mV/s; $NaIO_4$, 2 mM; $NaClO_4$, 2 mM; cell resistance, 1.0 kΩ). (b) Time series of current oscillation at U = -0.858 V.*

SPI images of the electrode/electrolyte interface, which were recorded during one current oscillation, are shown in Fig. 6.3. First we notice that the oscillation is clearly accompanied by pronounced changes in the optical properties of the interface, which give rise to a significant contrast in the series of images. Second, it is obvious that the oscillations are not completely homogeneous. The electrode is nearly uniform for low current densities. However, after the sharp increase in

current density, a horseshoe-like structure appears that slowly loses intensity as the current decreases, whereby during the final transition to the homogeneous state, one side of the horseshoe undergoes the transition to the passive state prior to the other side. In fact, under no conditions did we observe completely homogeneous oscillations. Instead, the described pattern was practically invariant under a parameter change. This impedes a clear cut distinction between truly self–organized structures and patterns that are induced by 'external inhomogeneities'. The inhomogeneities might be due to an inhomogeneous electrode surface, to non–uniformities in the transport conditions (recall that during the experiments the solution was slightly stirred by gas bubbles which might induce an inhomogeneous velocity field of the convective flow) or non-uniformities in the current flow through the electrolyte, or due to an asymmetric nonlocal coupling owing to the position of the RE (in our case, the RE was put closer to the side that is depicted left in the images in Fig. 6.4).

As for the question of the impact of the negative global coupling on pattern formation, we consider the image series depicted in Fig. 6.3 as a 'base sequence' and study how the pattern changes due to the presence of the negative global coupling. Since in all experiments with global coupling, the spatial symmetry was only broken along the longer direction of the electrode, whereas the emerging patterns were practically uniform along the short electrode direction, it is advantageous to represent the spatiotemporal dynamics in x–t plots, whereby each spatial profile represents the averaged SPI image intensity along the short direction of the electrode. For comparison, an x–t plot of two of the oscillations shown in Fig. 6.2b is depicted in Fig. 6.4 together with the corresponding time series of the current density. The second one of the oscillations represents the oscillation shown in Fig. 6.3. In this representation, the activation of the surface occurs nearly homogeneously, whereas the passivation seems to start at one end of the electrode and to propagate towards the other end. Furthermore, within the half in which the passivation starts, there is also a localized oscillation during the initial activation phase.

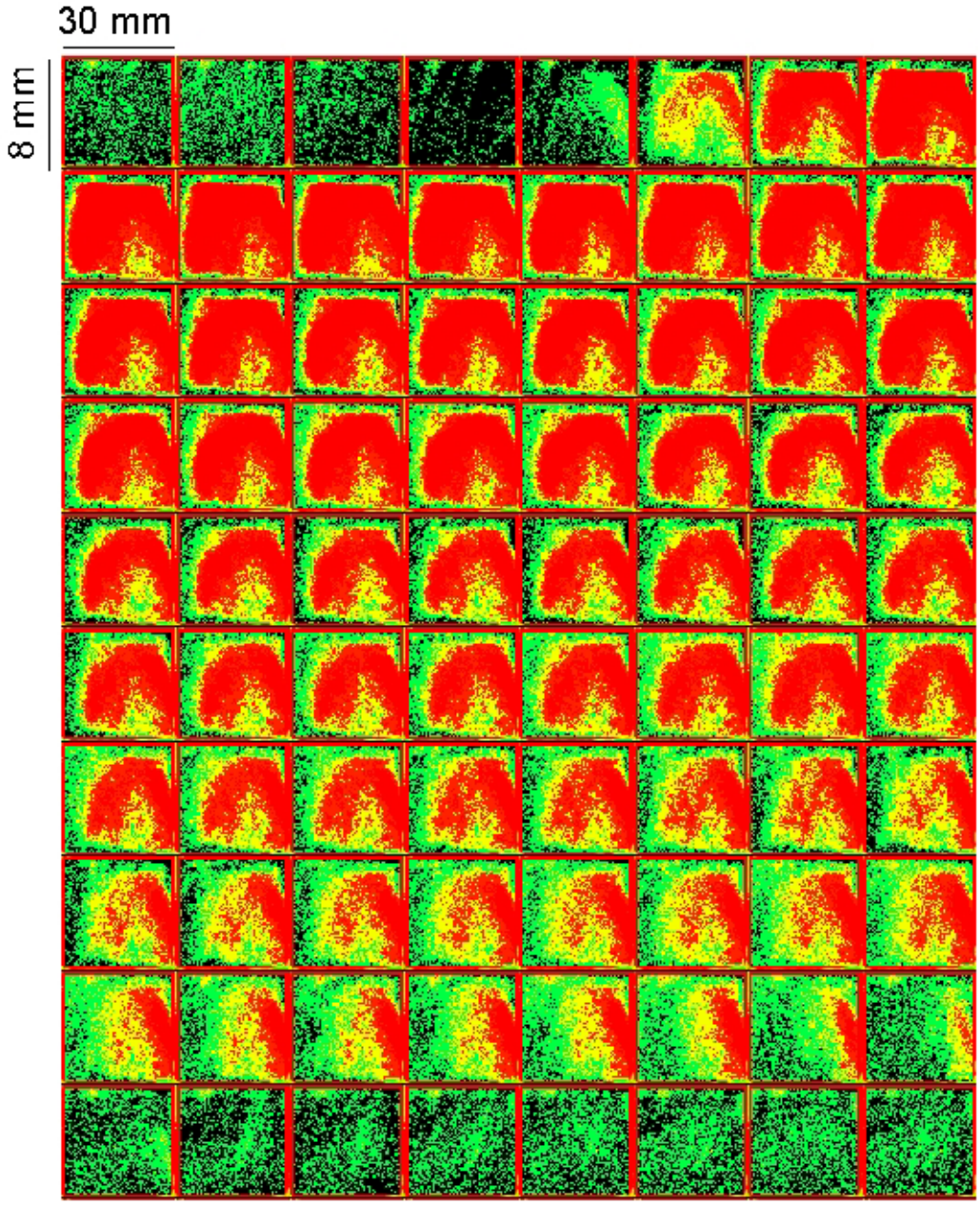

Figure 6.3: *Series of SPI images of the electrode surface during one of the current oscillations shown in Fig. 6.2b (note that the two directions of the electrode are displayed in different scales). The time interval between successive images is 50 ms. The whole images series corresponds to the 8 – 12 second time domain in Fig. 6.4.*

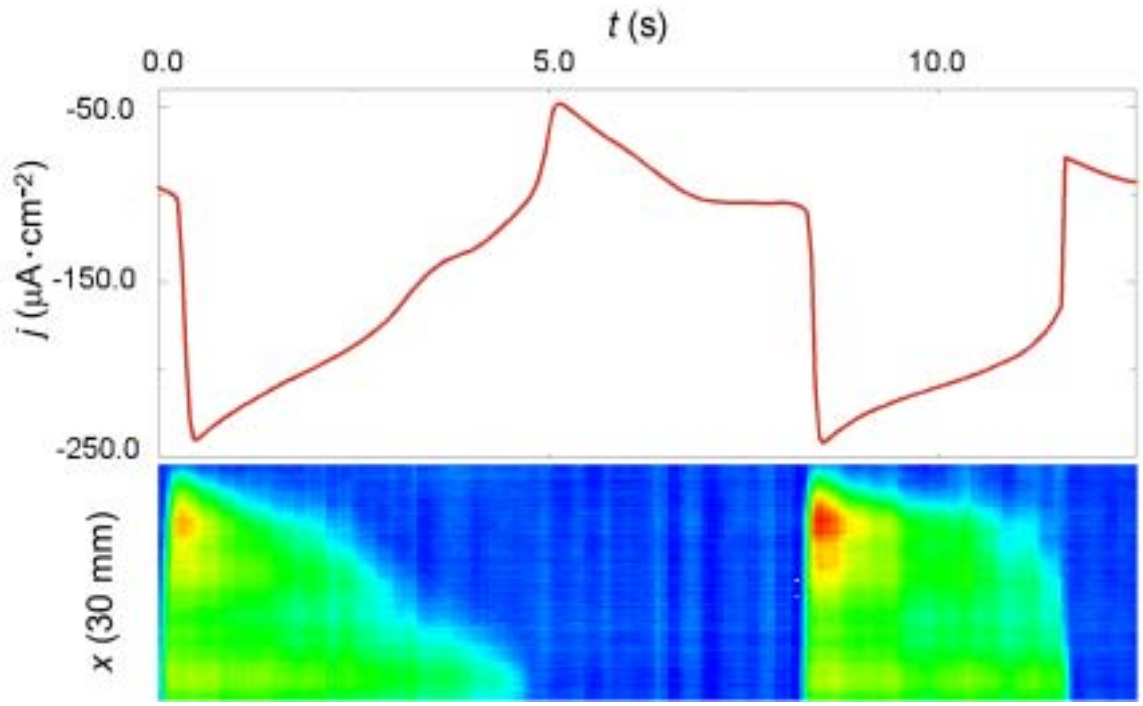

Figure 6.4: *X–t plot (bottom) of the SPI images taken during two of the oscillations shown in Fig. 6.2b and the corresponding time series of the current (top). The spatial profiles represent spatial averages over the short direction of the electrode.*

b. Periodate reduction system with the NID

The effect of the NID on the global, i.e., the homogeneous dynamics, is identical to the effect a reduced cell resistance has. This can be nicely seen when comparing the CVs depicted in Figs. 6.1 and 6.5. Both were obtained under identical conditions, except for the presence (Fig. 6.5) or the absence of the NID in series to the WE. (Note that the effective negative impedance of the NID is smaller than the cell resistance so that the total resistance is still positive.) For a lower total ohmic resistance in series to the interface (Fig. 6.5), the NDR region is still present, and oscillations occur around the NDR branch also during the potential scan. This is exactly the behavior that is common to all N-NDR systems. They exhibit a region of negative differential resistance for vanishing cell resistance (ohmic series resistance); this region becomes smaller as the series resistance is increased and oscillations develop around the NDR branch; for even larger series resistance the system becomes bistable and the NDR is not apparent anymore in a CV. Note, however, that in the periodate system oscillations were

only observed during voltage scans into the positive direction. For the generic N-NDR oscillator oscillations are expected to exist – at least in some interval of the series resistance – without this hysteresis. This indicates that the reduction of periodate on Au possesses a somewhat more complicated dynamics than the generic N-NDR oscillator. For the present question the detailed reaction dynamics is, however, not of importance and was, for this reason also, not further investigated.

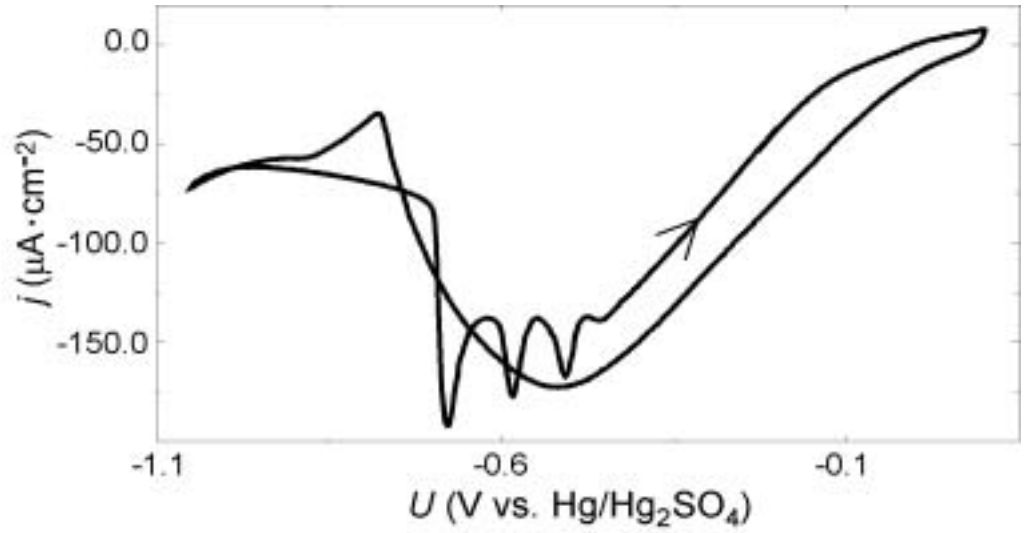

Figure 6.5: *Cyclic voltammogram of periodate reduction on a Au(111) film electrode in the presence of the NID (R_{NID} is adjusted to -1000 Ω) (scan rate, 50 mV/s; $NaIO_4$, 2 mM; $NaClO_4$, 2 mM; cell resistance, 1.0 kΩ).*

Fig 6.6 shows a series of SPI images that were recorded at a fixed value of the externally applied voltage during 5 oscillations of the current density. Clearly, the spatial behavior differs drastically from the one without the NID, which was discussed above (cf. Fig. 6.3). The electrode still takes on a quasi-homogeneous state in the current minimum of the oscillation, but the activation is restricted to only half of the electrode, whereby the two halves are activated alternatively. A complete spatiotemporal oscillation is thus composed of two oscillations of the global current density. The division of the electrode occurs along the long side, the short side being uniform except close to the edges where the electrode always takes potentials close to the passive state. The spatial symmetry breaking is thus restricted to one spatial dimension, the dynamics being consequently captured in an x–t plot.

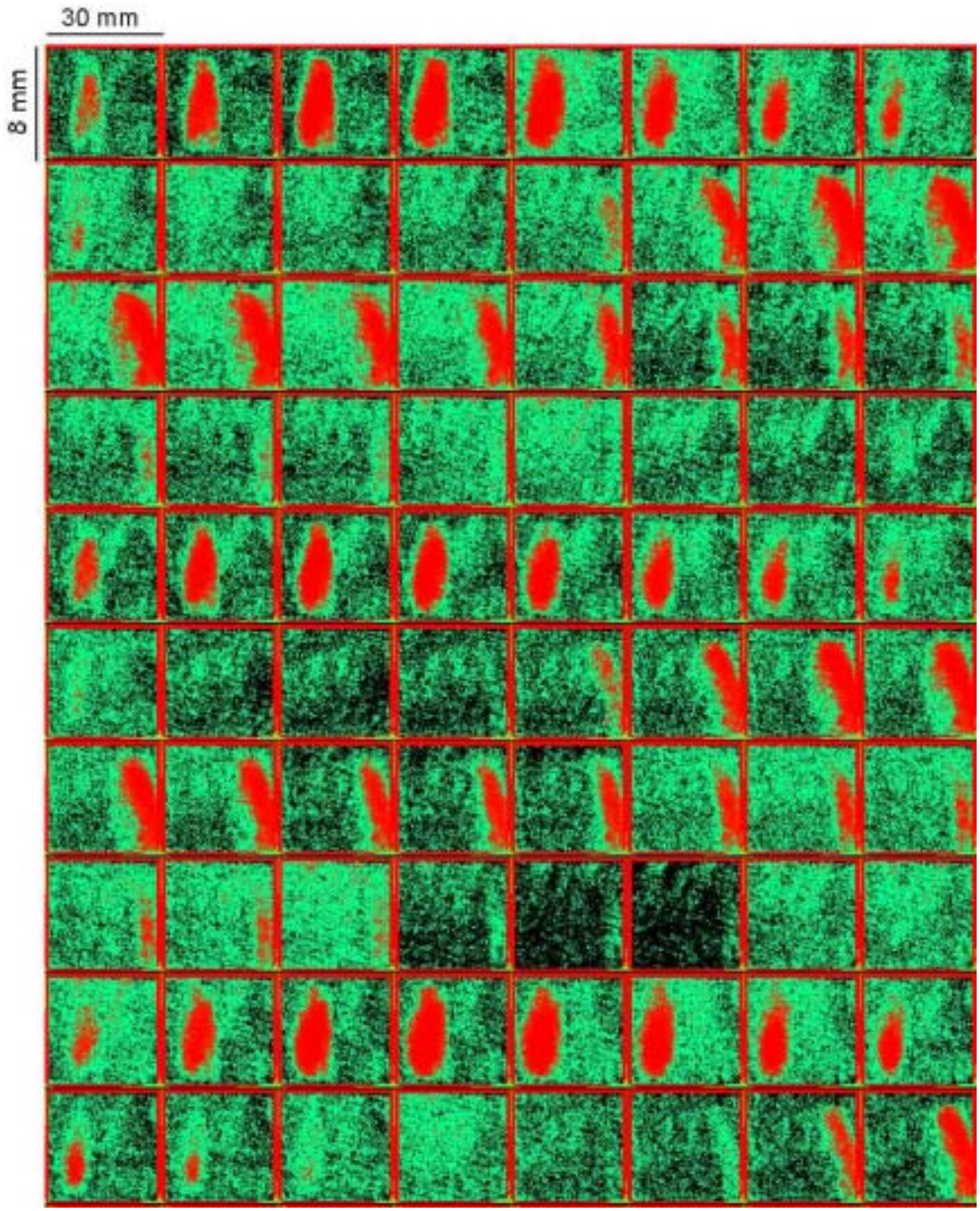

Figure 6.6: *SPI images of the Au(111) film electrode during periodate reduction in the presence of an NID (R_{NID} is adjusted to -800 Ω) giving rise to negative global coupling. (Time interval between successive images: 100 ms; externally applied voltage U = -0.571 V; electrolyte: 3 mM $NaClO_4$ and 2 mM $NaIO_4$; cell resistance, 1.0 kΩ.)*

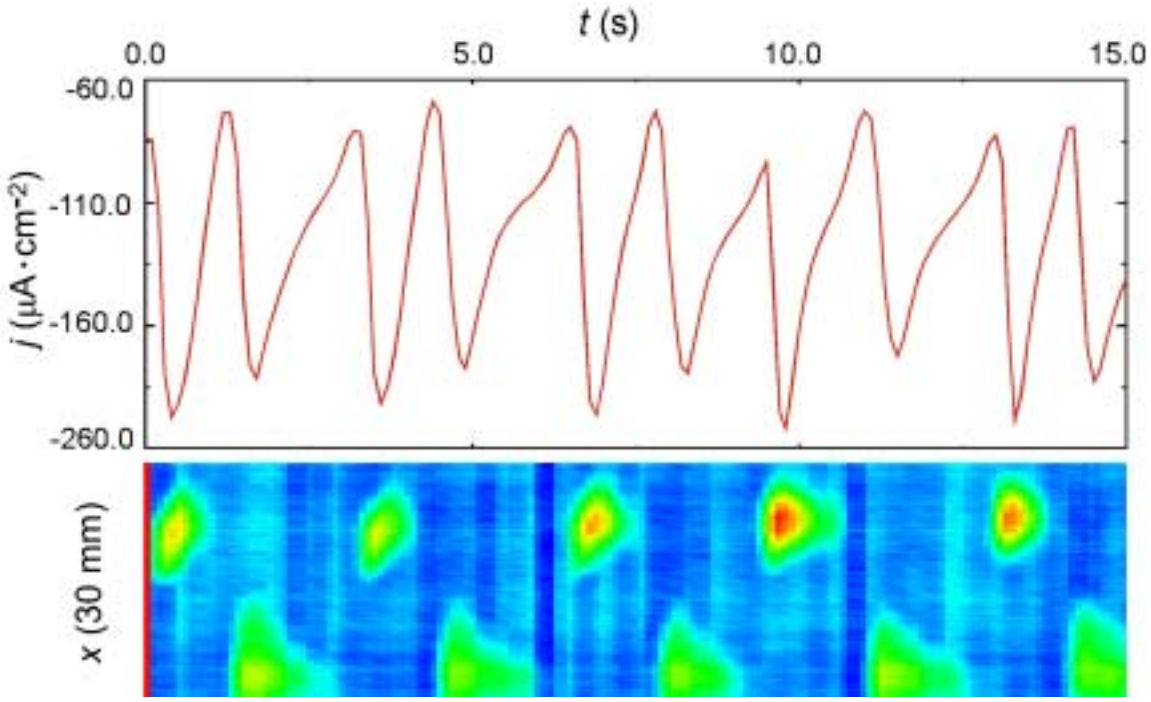

Figure 6.7: *X–t plot (bottom) of the SPI images and the corresponding time series of the global current (top). The conditions are identical with those in Fig. 6.6. The spatial profiles represent spatial averages over the short direction of the electrode.*

An x–t plot for the data that are partly shown in Fig. 6.6 is depicted in Fig. 6.7 for a longer time together with the corresponding time series of the global current. The spatial profiles again represent the spatial average over the short side of the electrode.

The alternate oscillations on the two sides are obvious. In this representation they resemble – somewhat distorted – standing waves. In the x–t representation it is also easy to realize that the oscillations on the two sides are not symmetric. This asymmetry also shows up in the current trace, which possesses a period-2 structure. While the basic symmetry breaking is clearly induced by the negative global coupling and a true self-organization phenomenon, the slight asymmetry of the oscillations on the two sides is most likely caused by an asymmetry in the

experimental setup as discussed above in the context of the spatiotemporal behavior without global coupling.

The symmetry breaking also occurs during a voltage scan. An overview of the different patterns that might establish at different values of the external voltage can be easily obtained when recording SPI images during a slow voltage scan. Such an experiment is shown in Fig. 6.8 and Fig. 6.9. Fig. 6.8 shows the anodic sweep of a cyclic voltammogram. It is obvious that when coming from the negative side, the oscillations apparently set in with a large amplitude. For more positive potentials the amplitude decreases slowly, the transition between the oscillations and the stationary state apparently occurring through a vanishing amplitude of the oscillations. This behavior is typical for a supercritical Hopf bifurcation, whereas the hard onset of the oscillations at the negative end can have different reasons. We will come back to this point below in connection with the simulations.

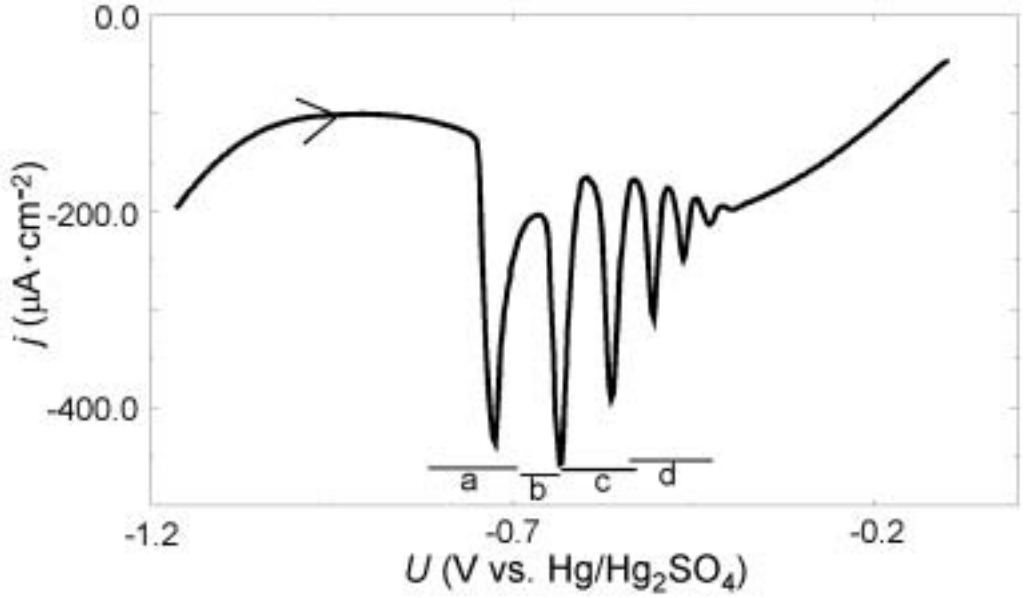

Figure 6.8: *The current–voltage curve during a positive potential scan in the periodate reduction system (scan rate, 50 mV/s; R_{NID}, -800 Ω; cell resistance, 1.0 kΩ; electrolyte: 3 mM $NaIO_4$, 2 mM $NaClO_4$). (Note: a,b,c and d label the potential regions where we observed the different patterns in Fig.6.9a,b,c,and d correspondingly.)*

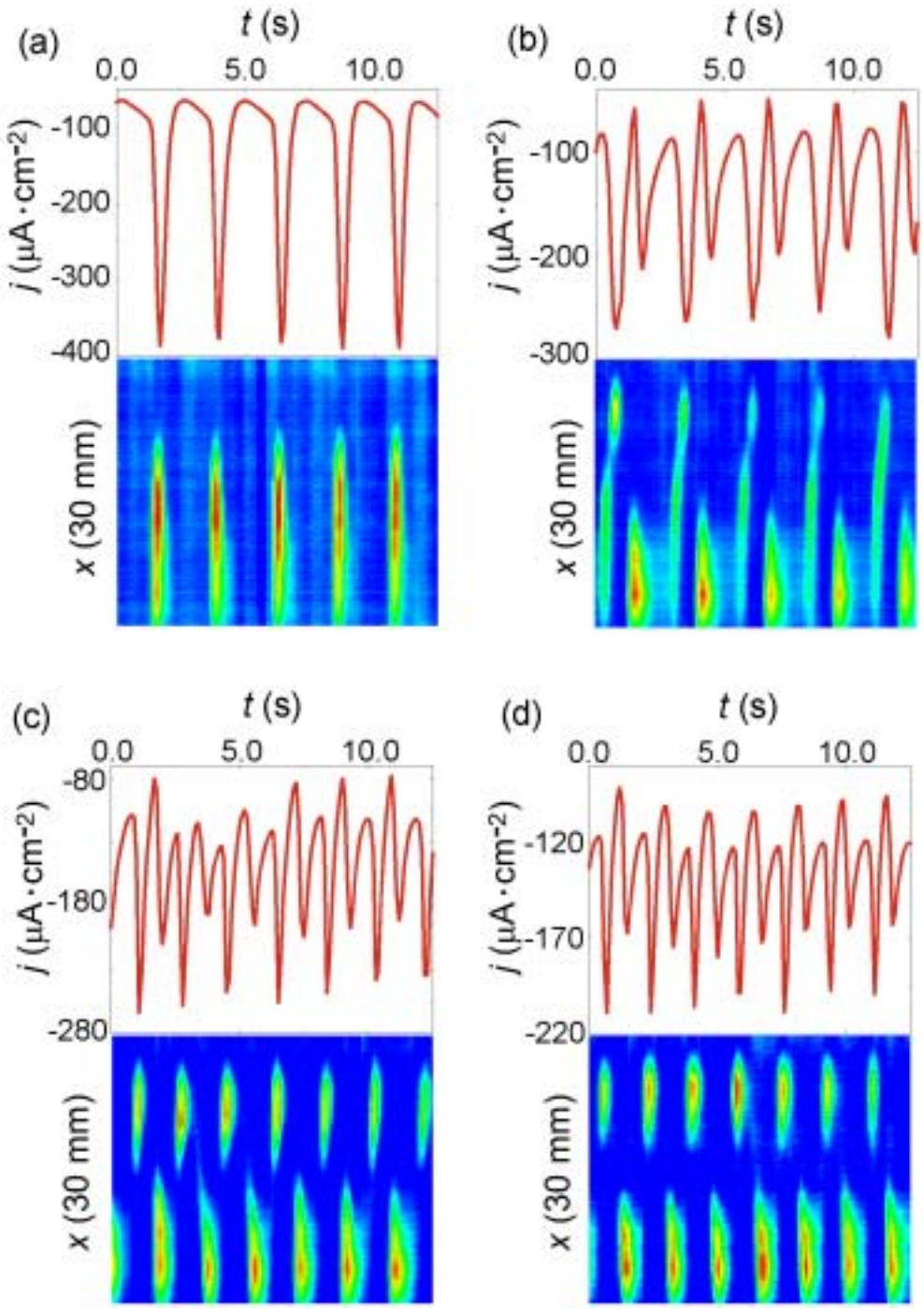

***Figure 6.9**: Pattern evolution during slow voltage scans (1 mV/s) in four different regions (a,b,c and d refer to those in Fig. 6.8) of the external voltage in the same system as in Fig. 6.8 (scan rate, 1 mV/s; R_{NID}, -800 Ω; cell resistance, 1.0 kΩ; electrolyte: 3 mM $NaIO_4$, 2 mM $NaClO_4$).*

Fig. 6.9 displays four x–t plots with corresponding time series of the global current that were recorded during a voltage scan in the anodic direction with 1 mV/s in four different regions of the external potential. The first set of data was obtained close to the negative end of the oscillation region (Fig. 6.9a). The current oscillations are simple periodic, relaxation-like and have an amplitude of more than 300 mV. The corresponding x–t plot exhibits oscillations that seem to be restricted to about 2/3 of the electrode and appear, different from the above example, for every oscillation of the current at the same side of the electrode. Again, here we cannot discriminate whether the partition of the electrode into two parts covering approximately 2/3 and 1/3 of the electrode, whereby one part is oscillating and the other part essentially stationary, is a true spatial symmetry breaking or whether it arises from an asymmetry in the setup implying that the oscillations in a perfect setup would be uniform.

The last x–t plot (Fig. 6.9d) was taken close to the positive end of the oscillatory region. It has the same characteristics that were discussed above for the stationary experiment (Fig. 6.7). The two halves of the electrode oscillate alternately, and the current oscillates with a period two. This behavior is robust in a wide voltage interval and is still found 100 mV more negative, as can be seen in the third spatiotemporal plot (Fig. 6.9c). In this set of data the oscillations are less regular than in the other sets displayed here. This is particularly obvious in the time series of the current. Experiments, in which the voltage was kept constant, showed that the irregularity is not linked to the slow variation of the voltage; rather, several tests strongly suggested that some unavoidable irregularities of the gas bubble stirring (which was necessary to obtain an appreciable current density and thus also to obtain oscillatory behavior) are responsible for them. In different voltage regions the influence of these irregularities varied greatly, depending on the robustness of the respective behavior, but perfectly regular oscillations over a long time were never found. This inhibited some quantitative measurements (e.g., to test for a hysteresis at the negative end of the oscillation region) but does not affect the principle occurrence of the phenomena discussed here.

Obviously, there is a qualitative transition between the simple periodic oscillations at the negative end of the oscillatory region and the period doubled behavior on its positive side. This transition is mediated via a mixed behavior which is depicted in Fig. 6.9b. There seems to be a pulse-like motion from the originally oscillating side to the other side, in between two of these pulses being an oscillation that is localized on the side that was originally oscillating. The corresponding current density exhibits a period-2 structure, the difference of the maximal and minimal currents in successive oscillations being more pronounced than in the case of the alternatively oscillating electrode halves. Furthermore, the current maxima are not as sharp. Correlating the time series and the spatial profiles, it becomes apparent that the longer time, in which the current density is high, results from the active pulse-like region which propagates to the other end.

6.3 Discussion

The results summarized in the preceding section clearly showed that the main effect of the negative global coupling is to induce a spatial symmetry breaking into one spatial dimension, namely the longer direction of the electrode. The symmetry breaking always leads to the partitions of the electrode into two parts, both parts oscillate with a phase shift of 180°. The spatiotemporal dynamics closely resembles a standing wave.

As mentioned in the introduction of this chapter, all experiments on the impact of a negative global coupling on the spatiotemporal dynamics of electrode reactions have been carried out so far with quasi-1D electrodes, and with the exception of one example, in which a thin ribbon was used [96] and which leads to further complications due to the intrinsically higher current density at the edge [97], ring electrodes were employed. In these experiments, there were two dominating patterns: standing waves and pulses [19, 20, 22]. Both patterns could be shown to result from a nontrivial Hopf bifurcation, in which a complex conjugate pair of eigenvalues that correspond to the eigenmodes with the wave number 1, cross the real axis, while all other eigenvalues are still negative. Hence, when passing the Hopf bifurcation, instead of the development of uniform oscillations (in this case, the eigenvalues corresponding to the homogeneous

mode had to become unstable first) the lowest spatial eigenmode starts to oscillate. For 1D ring electrodes the eigenmodes are Fourier modes. This means that for each wave number there are two degenerate eigenmodes, a sine and a cosine mode. Somewhat simplified, the formation of the standing waves could be thought as the result of the excitation of just a sine or a cosine mode, whereas a pulse results when both, sine and cosine modes are excited simultaneously.

Transferring these arguments to our experiments and for a moment disregarding the second spatial dimension, the electrode should be modeled as a one-dimensional domain with *zero-flux boundary conditions*. The respective eigenmodes are cosine modes, the lowest one corresponding to a cosine running between 0 and 180°. A nontrivial Hopf bifurcation with n = 1 should thus give rise to a standing wave-like behavior. This is at least qualitatively in agreement with the observation. Note, however, that close to the bifurcation the standing wave oscillation has its maxima at the edges. In the experiments the edges clearly showed a much smaller amplitude. Here, again, experimental limitations seem to come into play. At the transition between the electrode and the cell, the opening of the cell wall formed walls that were nearly perpendicular to the electrode. When the electrode is placed in such a 'box', the transport to the edges of the electrode is worse than to the center. Thus, close to the edges discrepancies between an idealized behavior as assumed in the above considerations are to be expected.

The experiments motivated a theoretical study on pattern formation in a generic N-NDR system with negative global coupling [31]. Since there are profound similarities between the simulations and the experiments, the main theoretical results shall be summarized. Fig 6.10 shows a calculated polarization curve. The dashed curve between A and C denotes the unstable stationary state; it exhibits a negative differential resistance. In an experiment this part of the polarization curve would not be accessible. Rather, oscillations, whose amplitude reach the thick line connecting points C, B and A, would be seen. When increasing the external potential from negative values, the oscillations set in apparently with a large amplitude. This is in perfect agreement with the experimental results. A bifurcation analysis revealed that the bifurcation in the homogeneous model is a

supercritical Hopf bifurcation, but with an extremely sharp increase in amplitude close to the bifurcation. This means that the oscillations emerge respectively die without hysteresis when sweeping across the bifurcation point from the cathodic and anodic direction.

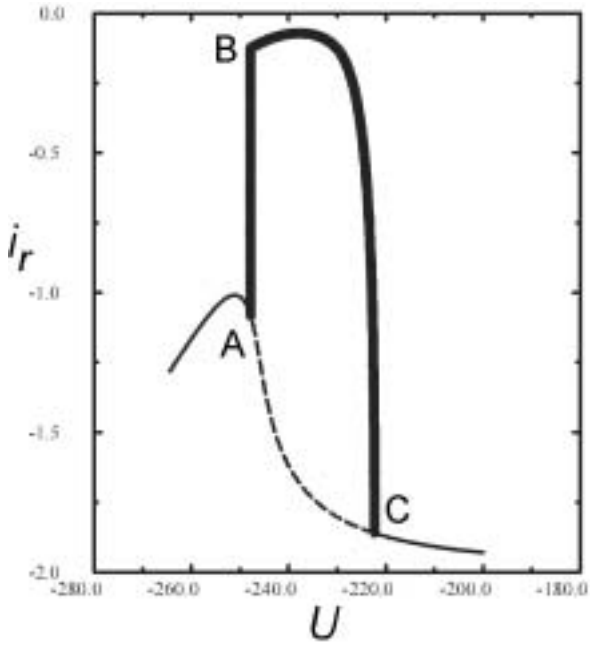

Figure 6.10: *Calculated bifurcation diagram of a generic N-NDR model [31].*

Without negative global coupling or a low strength of the negative global coupling, the model exhibits spatially homogeneous oscillations (Fig. 6.11a). For a large value of the negative global coupling, however, spatially inhomogeneous oscillations exist in the entire parameter interval. At the positive end of the oscillatory region, the oscillations are born in a nontrivial Hopf bifurcation, in which a pair of complex conjugate eigenvalues corresponding to n = 1 changes sign, giving rise to standing waves. This confirms the above discussion on how the standing waves might emerge. Standing wave-type oscillations were found in a wide voltage interval (Fig. 6.11b). Close to the negative end of the oscillatory region, the standing waves transformed into an oscillating, asymmetric structure, which can be described best as a homogeneous oscillation in one half of the electrodes which sends out pulses into the second half (Fig. 6.11c).

(a)

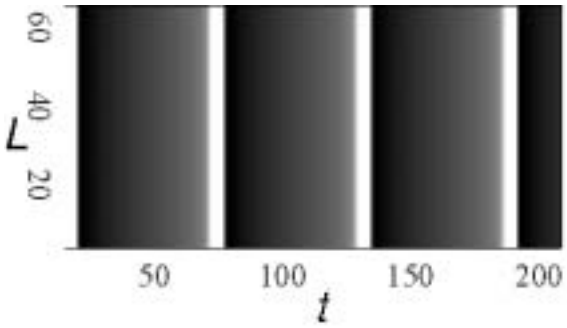

(b)

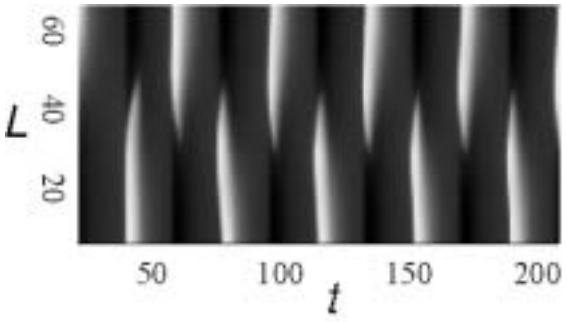

(c)

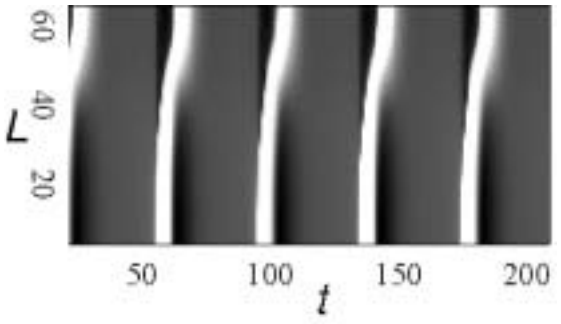

Figure 6.11: *Spatiotemporal dynamics of a generic N-NDR model [31]: (a) Without negative global coupling; only spatially uniform oscillations were found. (b) With strong negative global coupling; starting at the positive onset of the oscillations, standing waves with n = 1 exist in a wide voltage interval. (c) With strong negative global coupling; close to the negative end of the oscillatory region, the oscillations become spatially asymmetric.*

Comparing the calculations with the above discussed experiments, there are striking corresponding features, but also some discrepancies. The prevailing behavior in both, experiments and simulations, is the existence of standing waves with wave number 1 in a wide voltage interval starting at the positive end of the

oscillatory region. The simulations confirm that these patterns emerge due to the existence of the negative global coupling and that the standing waves are born in a nontrivial Hopf bifurcation. Note, however, that in the calculations and in agreement with the considerations above, the standing waves possess their maximal amplitude at the edges while it is somewhere between 1/8 and 1/4 away from the edge in the experiments. It seems to be very likely that this discrepancy results from a lower transport of periodate to the edges of the electrode compared with that to its central part.

The spatiotemporal dynamics in the standing wave regime possesses a symmetry (which is not perfect in the experiments due to the presence of inhomogeneities): The pattern is invariant upon reflection at the center of the electrode followed by a phase shift of 180° of the local period in time. This symmetry is broken, again in the experiments as well as in the simulations, close to the negative end of the oscillatory region. Moreover, in simulations and experiments the resulting dynamics exhibits oscillations that emerge nearly homogeneously over about one half of the electrode and send out a pulse in the second half. Recalling that the model does not include any specific kinetics of the periodate reduction but describes the reaction current by a polynom of third degree, the correspondence of this subtle feature impressively confirms that these features are generic and should exist in any N-NDR oscillator with negative global coupling.

However, there are also two fundamental discrepancies between the calculated dynamics and the experimental results. In the experiments between two of the above described asymmetric oscillations, there is a localized oscillation on the side on which the asymmetric oscillation emerges. Such a more complex succession of 'asymmetric' and localized oscillations has never been observed in the cited simulations. Moreover, in the immediate neighborhood of the negative end of the oscillatory regime, simple periodic oscillations were found in which about 2/3 of the electrode took part, the remaining third being practically stationary. This third was not centered around the middle of the electrode. Rather, it was covering the area against one edge of the electrode. There are different possible explanations of these discrepancies. First, the simulations were carried out varying the parameters, and most importantly, the strength of the

negative global coupling in finite steps over a wide regions. With such a procedure, it is in principle impossible to exclude the existence of some patterns completely. However, it can certainly be concluded that if the generic N-NDR model with negative global coupling also possessed such solutions, they would occur in smaller parameter intervals than in the experiments. This explanation thus seems to be somewhat unlikely. Second, we can also not exclude that the patterns are caused by a reaction kinetics that is more complicated than the one of the generic N-NDR model. However, there is another discrepancy (seems to be more decisive) between the simulations and the experiment, the positioning of the RE. In the modeling it was assumed that the RE is positioned on an equipotential plane parallel to the WE. In this way, an influence of an asymmetric negative coupling due to the RE could be excluded. Unfortunately, such an idealized situation does not exist in the experiment. Instead, the RE was located approximately at the height of the CE and close to one side of the WE. This implies that the potential drops from the RE to different positions on the WE are different. Consequently, there is a slight gradient in the effective resistance which causes a slight shift in the homogeneous dynamics. Clearly, the impact of the gradient is more pronounced close to the border of the oscillatory region and well in the oscillatory region. In particular, in a small voltage interval, part of the electrode might be oscillatory, while the other one is not. Simulations with an asymmetrically placed RE were carried out by Birzu et al. [98] using a model describing metal dissolution and a one-dimensional ribbon electrode. Since the reaction dynamics does not correspond to the generic N-NDR model and the boundary represents a metal-insulator transition which deviates greatly from the zero-flux boundary that corresponds to the experimental situation, the simulations cannot directly be used to explain the experiments. However, it is remarkable that these simulations exhibit a pattern, in which one side of the electrode oscillates with twice the frequency of the other side. This result is a hint that the position of the reference electrode causes the main qualitative differences in the dynamic behavior between the experiments and the above cited simulations. In view of the discussion of the impact of the asymmetrically placed reference electrode on the dynamics, we would like to emphasize again that the symmetry breaking from the symmetric standing waves to the asymmetric oscillations with pulse emission were also found in the simulation with a

perfectly symmetric geometry and is thus not caused by the unavoidable non-uniformities present in any experiment. The discussion also shows how intricate the interaction between reaction kinetics, negative global coupling and non-uniformities might be, which makes an interpretation of the origin of the pattern without accompanying calculations nearly impossible.

Finally, we would like to comment on a last issue. The experiments discussed above were carried out with 2D rectangular electrodes. However, the spatial symmetry breaking induced by the negative global coupling took place exclusively in one spatial dimension, namely the longer one. For this phenomenon there are at least two possible explanations: (a) Either the critical length, beyond which the system is too small to allow for a nontrivial Hopf bifurcation, is larger than the small side of the electrode, or (b) the uniform surface could become unstable with respect to a symmetry breaking in either of the two spatial dimensions. The basin of attraction of the solution that exhibits a symmetry breaking into the smaller direction is, however, much smaller such that it is much less likely to occur. Schöll and coworkers [99] performed calculations on pattern formation in 2D semiconductor electrodes in the presence of a global coupling. They found that if the one-dimensional symmetry breaking can occur in either of the directions, also so-called edge oscillations are stable, which can be easiest described by an oscillation of one quarter of the electrode, i.e., a truly two-dimensional oscillating pattern. Our experiments showed that, at least for these largely different lengths of the two electrode sides, edge oscillations are very unlikely. Calculations with the generic N-NDR model and a two-dimensional electrode geometry are necessary to test whether this type of patterns exists at all in electrochemical systems and in which parameter range and for which aspect ratio of the electrode it is to be expected.

6.4 Summary

In this chapter, we described pattern formation on a rectangular gold film electrode during periodate reduction in the presence of a negative global coupling. The periodate reduction is a typical N-NDR oscillator; the studies are thus representative for all N-NDR systems. The negative global coupling was

accomplished using an electronic device which acts like a negative ohmic resistor. This is the only way in which a strictly negative global coupling can be imposed on an electrochemical cell (making RE close to WE is an alternation to induce the negative global coupling only for ideal 1D ring electrodes). Its relevance lies in the fact that also the 'automatic IR compensation' that many commercial potentiostats offer, acts like a negative ohmic resistor in series to the WE. From a critical coupling strength on, the negative global coupling leads to a spatiotemporal symmetry breaking, thus impeding the existence of uniformly reacting electrodes. In wide parameter regions, standing waves with a wave number 1 were obtained. Close to the negative edge of the oscillatory region, less symmetric spatiotemporal dynamics existed. A comparison with existing simulations showed that the basic features of the patterns are due to the negative global coupling and exist also in perfectly homogeneous systems. The fine structure of the patterns was not reproduced in those simulations and is most likely due to unavoidable non-uniformities in the experimental setup.